

Determination of tensile crack bridging of PCM-concrete interface subjected to fatigue loading by means of bending test

Dawei Zhang^{*}, Hitoshi Furuuchi^{**}, Akihiro Hori^{***}, Fujima Seiji^{****}, Tamon Ueda^{*****}

^{*} Lab of Engineering for Maintenance System, Division of Built Environment, Hokkaido University, M.E.

^{**} Lab of Engineering for Maintenance System, Division of Built Environment, Hokkaido University, Dr.E.

^{***} Special Additives Dept., DENKA Chemicals GmbH, Sales Manager, Dr.E.

^{****} Hardloc Production & Technical Support Section, Denki Kagaku Kogyo CO.,Ltd., Assistant Manager.

^{*****} Lab of Engineering for Maintenance System, Division of Built Environment, Hokkaido University, Dr.E.

In this paper, a simple and handy test method for determination of the tensile crack bridging law of PCM-concrete interface is proposed. Based on the fatigue failure mechanism of PCM-concrete interface that is governed by crack propagation as the result of interface bridging degradation, the J-integral method proposed for determining the tension softening relation of concrete under static loading is modified to determine the PCM-concrete interface tensile stress degradation relation. The derived degradation relation is compared to that of normal concrete under cyclic uniaxial tensile tests, and it can be found that the PCM-concrete interface has higher degradation rate so that more attention should be paid to the PCM-concrete interface during the design of PCM-retrofitted structures under fatigue loading.

Keywords: PCM-concrete interface, Fatigue bending test, stress degradation law, energy equivalence

1. BACKGROUND

Polymer cement mortar (PCM) overlay method (PCM retrofitting method) is used to increase the load capacity and environmental resistance of bridge decks. In light of the weak bond strength of normal cement based materials, PCM offers a good compromise in terms of cost and behavior. The PCM retrofitted highway or bridge deck are expected to resist millions of cycles of repeated axle loads from passing traffic during their service life. Subsequently, PCM based repairs have sometimes posed a problem due to their debonding. Debonding can start from any discontinuity (boundary, joints or crack cutting the overlay), often with a lifting of the edges of the debonded area. This induces new cracks which accelerate the damage process, and new repair work is needed¹⁾. As a result, there is increasing interest in better knowledge to predict the behavior of PCM-concrete interface under cyclic loading and to find solutions to ensure their durability.

Although there are many studies reporting the improvement in the mechanical properties of PCM and the failure mechanism of them under static and cyclic loading conditions were presented²⁾, there have been few studies related to PCM-concrete interface properties and failure mechanisms under a fatigue loading condition. Fatigue life prediction and the design of PCM repaired

structures can so far only be performed through an empirical approach. The investigations on the fatigue properties and failure mechanisms of PCM-concrete interface are necessary for proposing a proper repair method. This leads to the necessity of the development of an analytical tool that is applicable to the prediction of interface fatigue performance and to the design of structural repairs in the future.

Various approaches have been used in the fatigue life assessment of structural elements. A widely accepted approach for engineering practice is based on empirically derived S-N diagrams, also known as Wöhler curves. This approach provides a relation between maximum stress or stress amplitude and the number of load cycles to failure. However, it does not allow us to describe the softening behavior of material because of the applied force control, which consequently leads to unstable crack propagation. The deformation controlled uniaxial tensile test on notched concrete prism is a more direct way to investigate the material property under cyclic loading condition. However, such a test procedure requires a very specific and precise way to carry out in comparison with bending test, which is normally applied to provide data for the verification of the material law. Recently, a fatigue analysis method combining the bridging stress degradation law under cyclic load and FEM analysis is raised by Peerapong et al³⁾. In this method, the S-N relation from the bending tests is introduced with the fatigue analysis model to determine the fatigue bridging stress degradation

relation and the evolution of mid-span deflection is selected for the verification. The experiments are easier to be conducted but the analysis procedure may take time.

Starting with the J-integral based method by Li et al.⁴⁾, a series of methods based on energy balance have been proposed for determining the tension softening curve of concrete: the new J-integral based method⁵⁾, the modified J-integral method⁶⁾, and new method proposed by Niwa⁷⁾. By using J-integral method, the tension softening diagrams can be determined from a single beam specimen. Only the load, the load point displacement and the crack opening at the notch tip are necessary to be measured. It has been proved that the J-integral method is applicable to static tension softening relation of PCM-concrete interface. In this study, the J-integral method based on load controlled bending tests together with bridging degradation theory are introduced to determine the bridging stress degradation relation of PCM-concrete interface.

2. FATIGUE MODEL

2.1 Mechanism of fatigue crack growth in PCM-concrete interface

For PCM-concrete cold-joint interface, the material phases can broadly be classified as cement (in concrete or PCM) paste and aggregates, as well as the interfaces between aggregate and hydrated cement paste. The fatigue loading causes these physical phases to undergo microscopic changes, such as opening and growth of bond cracks, which exist at the interfaces between coarse aggregate and hydrated cement paste even prior to the application of load⁸⁾. These microscopic changes in turn cause detrimental changes in macroscopic material properties. Typically, the aggregate bridging force decreases with number of cycles because of the interfacial damage or aggregate breakage⁹⁾. Subsequently, the crack propagates both by increasing length and width with the increase of applied loading cycles until the equilibrium cannot be satisfied with further crack propagation. At this moment, the structure fails, and it defines the fatigue life. This mechanism is so called "Bridging Stress Degradation" and the PCM-concrete interface degradation law is considered the essential cause of crack propagation and needs to be clarified. Based on the above discussions, some basic assumptions for fatigue modeling can be stated:

1. After a dominant fatigue crack is created, the bridging behavior within the fracture zone is governing the rate of fatigue crack development.
2. The stress at the crack tip remains constant and is equal to the material tensile strength.
3. Material properties outside the fracture zone are unchanged during fatigue loading.

The J-integral method combines the fictitious crack model proposed by Hillerborg¹⁰⁾ with energy equivalence assumptions and has been applied to static analysis procedures. In the development of the fatigue analysis method, the failure of ordinary cementitious

materials, such as plain concrete and PCM-concrete interface, under fatigue flexure or fatigue tension is governed by the initiation and the propagation of a single localized crack; therefore, the fictitious crack is appropriate and enough for representing the crack and the failure mechanism. In order to correlate the J-integral method and fatigue analysis through energy equivalence concepts and to predict the crack development in PCM-concrete interface, the following additional assumptions may be noted:

4. The energy applied for the increment of deflection at loading point is totally absorbed for the fictitious crack propagation synchronously.
5. The crack propagation under fatigue loading is regarded as slow crack propagation under static loading. Only the energy applied during the deflection increment corresponding to the increments of crack length and width is taken into account, ignoring the energy corresponding to the overlapped part between adjacent hysteretic loops (see Fig.1).

2.2 Bridging model of PCM-concrete interface under tension fatigue

(1) Monotonic tension

The roughness of the joint surface, the mix proportions of substrate concrete and the construction method are the main factors affecting the bond properties of PCM-concrete interface. In the present investigation, an empirical model based on the J-integral method proposed by Zhang¹¹⁾ will be adopted. In this model the PCM-concrete interface tension softening relation is expressed as a function of the interface roughness, substrate concrete compressive strength and the crack mouth opening displacement (CMOD) based on the analysis of experimental data.

$$\left. \begin{aligned} \frac{\sigma}{f_{ii}} &= \left\{ 1 + \left(\frac{c_1 \cdot w}{w_c} \right)^3 \right\} \exp\left(\frac{-c_2 \cdot w}{w_c} \right) - \frac{w}{w_c} (1 + c_1^3) \exp(-c_2) \\ c_1 &= 2.46 \\ w_c &= 0.15 \text{ mm} \quad \text{if } (f'_c < f'_{PCM}) \\ c_1 &= -4.74R_a^2 + 9.24R_a - 2.18 \\ G_{fi} &= f'_{PCM} (1.32R_a + 0.08) \\ w_c &= \frac{5.14G_{fi}}{f_{ii}} \text{ mm} \quad \text{if } (f'_c \geq f'_{PCM}) \end{aligned} \right\} \quad (1)$$

where f_{ii} is interface splitting tensile strength, R_a is the interface roughness calculated based on JIS Standard¹²⁾, c_2 is taken as 6.93 and c_1 is a function of R_a , w_c corresponds to the crack opening when the stress has dropped to zero, G_{fi} is the interfacial fracture energy expressed as a function of compressive strength of PCM and interface roughness.

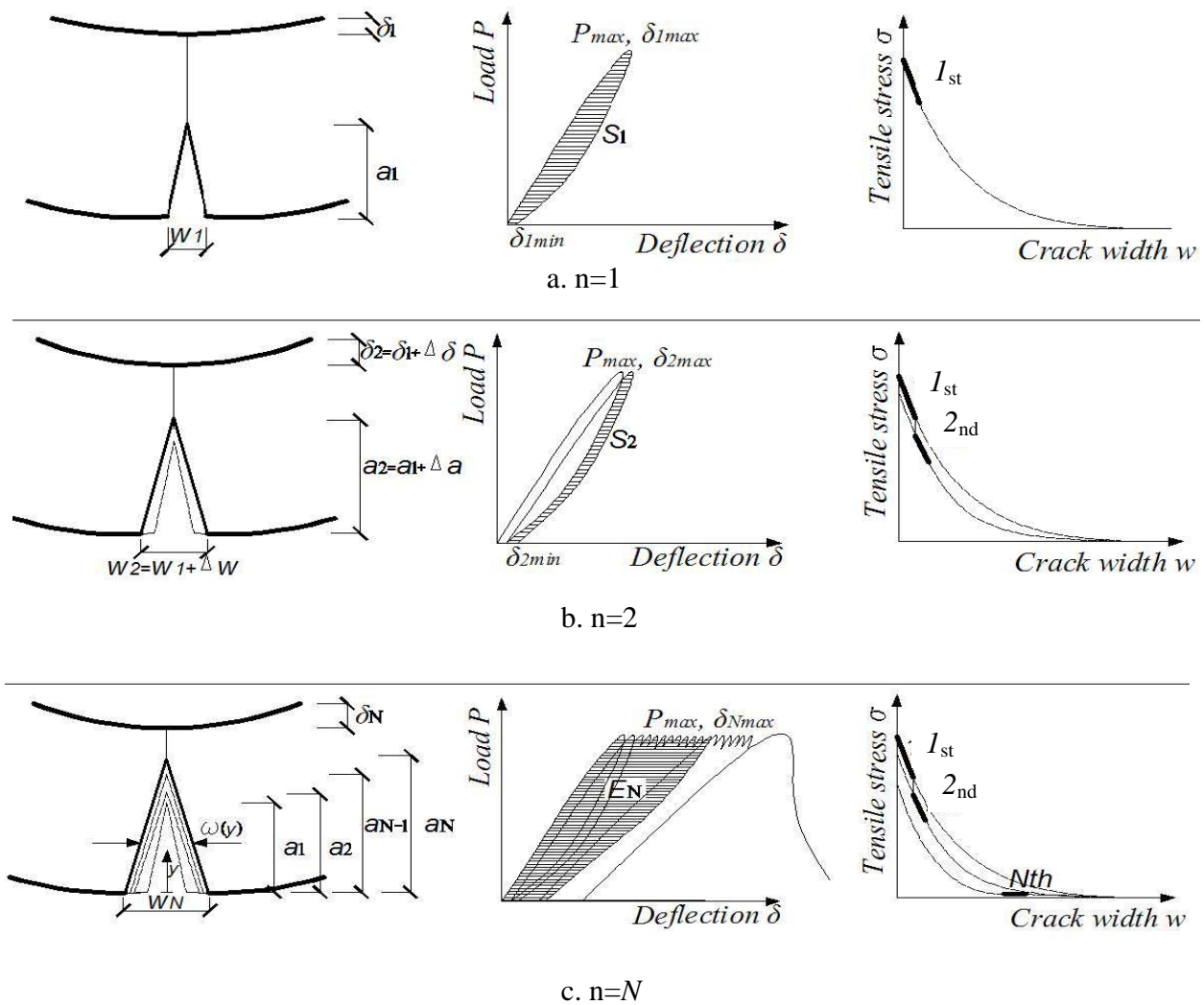


Fig. 1 Procedure of fatigue crack analysis

(2) Cyclic tension

Degradation of aggregate bridging of concrete under cyclic uniaxial tension has been studied by researchers in last two decades^{9, 15, 16, 17}. By analyzing the experimental data, it is concluded that the bridging stress degradation relation of cementitious materials depends on two main parameters corresponding to maximum crack opening w as the maximum crack width corresponding to the zero load, and number of cycles, N . It can be expressed as:

$$\left. \begin{aligned} \frac{\sigma_N}{\sigma_1} &= 1 - (k_1 + k_2 w) \log N \\ \text{for } (k_1 + k_2 w) \log N &< 1 \\ \frac{\sigma_N}{\sigma_1} &= 0 \\ \text{for } (k_1 + k_2 w) \log N &\geq 1 \end{aligned} \right\} \quad (2)$$

where σ_N and σ_1 represent bridging stress at N -th cycle and first cycle, respectively. σ_1 is given by Eq.(1); and k_1 and k_2 are degradation factors, which reflects the rate of aggregate bridging degradation.

3. PROCEDURE OF FATIGUE ANALYSIS

The procedure of fatigue life analysis is shown by a simple supported composite beam subjected to a fatigue load.

For a given maximum and minimum flexural fatigue load level, P_{max} and P_{min} , during the loading process in the first cycle, a crack initiates with maximum length a_{1max} and width w_{1max} , and the deflection experiences the maximum value δ_{1max} as shown in Fig 1.a. The bridging law without stress degradation ($N=1$) together with numerical integration method can be used to calculate the unit energy consumption of fictitious crack as:

$$e_1(w) = \int_0^w \sigma_1(\omega) d\omega \quad (3)$$

During the unloading process, a part of the external energy accumulated in other portions besides the fictitious crack will be released and there is a residual deflection $\delta_{1\min}$ in the fully unloaded state. Therefore, to properly evaluate the energy consumed in the fictitious crack, the amount of elastic energy released must be excluded. The energy applied for the fictitious crack increasing from zero to width $w_{1\max}$ during the first cycle is calculated as:

$$E(w_{1\max}) = \int_0^{\delta_{1\min}} P(\delta) d\delta \quad (4)$$

which equals to the area S_1 of the hysteretic loop of first cycle as shown in Fig.1.a

When the crack experiences the second cycle of load, the transferred stress across the crack reduces due to the deterioration of material constituent on the crack plane. The equilibrium can not be maintained with the degraded bridging stress distribution of the cracked area when CMOD reaches $w_{1\max}$. Therefore, the existing crack propagates with additional length Δa to $a_{2\max}$ and additional width Δw to $w_{2\max}$, and the deflection increases from $\delta_{1\max}$ to $\delta_{2\max}$. The bridging laws with $N=2$ and $N=1$ will be used in the old fracture zone and the newly developed fracture zone, respectively. The unit energy consumption of old fracture crack zone can be expressed as:

$$e_2(w) = \int_0^{w_1} \sigma_1(\omega) d\omega + \int_{w_1}^w \sigma_2(\omega) d\omega \quad (5)$$

The energy consumed for the CMOD increasing from $w_{1\max}$ to $w_{2\max}$ is calculated as:

$$E(\Delta w) = \int_0^{\delta_{2\min}} P(\delta) d\delta - \int_0^{\delta_{1\min}} P(\delta) d\delta \quad (6)$$

which represents the area S_2 as shown in Fig1.b . At this stage, the total energy consumed for CMOD increasing from zero to $w_{2\max}$ is calculated as

$$E(w_{2\max}) = E(w_{1\max}) + E(\Delta w) \quad (7)$$

which is equal to accumulation area of S_1 and S_2 .

The procedure will be continued with the extension of crack proceeds until the load capacity starts to drop with increasing crack length. At this stage, the composite beam is considered to have failed in fatigue. According to this procedure, for the N -th load cycle, the fracture history zone will be divided into N sections with different fatigue history, ranging from 1 to N cycles. The total energy consumed for CMOD increasing from zero to $w_{N\max}$ corresponds to the area enclosed by envelope

curves of load-deformation diagram and the unloading curve of last cycle with horizontal coordinate axis. The unit energy consumption of fictitious crack during this process can be expressed as:

$$e_N(w) = \int_0^{w_1} \sigma_1(\omega) d\omega + \int_{w_1}^{w_2} \sigma_2(\omega) d\omega + \dots + \int_{w_{N-1}}^w \sigma_N(\omega) d\omega \quad (8)$$

where w_1, w_2, \dots, w_{N-1} represent the history of crack width at each cycle.

As indicated in Fig.1.c, when the fictitious crack length is a_N and the fictitious CMOD is $w(y)$, the following relation can be obtained.

$$\omega(y) = wy / a_N \quad (9)$$

$$dy = -(a / w) d\omega$$

Then, the energy E_N which is consumed in this portion after N cycles of load can be calculated as follows:

$$E_N(w) = b \left[\int_0^{a_1} e_N(\omega) dy + \int_{a_1}^{a_2} e_{N-1}(\omega) dy + \dots + \int_{a_{N-1}}^{a_N} e_1(\omega) dy \right]$$

$$= b \left[\int_{w(1-\frac{a_1}{a_N})}^w e_N(\omega) \frac{a_N}{w} d\omega + \int_{w(1-\frac{a_2}{a_N})}^{w(1-\frac{a_1}{a_N})} e_{N-1}(\omega) \frac{a_N}{w} d\omega + \dots + \int_0^{w(1-\frac{a_{N-1}}{a_N})} e_1(\omega) \frac{a_N}{w} d\omega \right]$$

$$= \frac{ba_N}{w} \left[\int_{w(1-\frac{a_1}{a_N})}^w e_N(\omega) d\omega + \int_{w(1-\frac{a_2}{a_N})}^{w(1-\frac{a_1}{a_N})} e_{N-1}(\omega) d\omega + \dots + \int_0^{w(1-\frac{a_{N-1}}{a_N})} e_1(\omega) d\omega \right] \quad (10)$$

From Eq. (10), the following relationship can be derived

$$\int_{w(1-\frac{a_1}{a_N})}^w e_N(\omega) d\omega + \int_{w(1-\frac{a_2}{a_N})}^{w(1-\frac{a_1}{a_N})} e_{N-1}(\omega) d\omega + \dots + \int_0^{w(1-\frac{a_{N-1}}{a_N})} e_1(\omega) d\omega = \frac{w}{ba_N} E_N(w) \quad (11)$$

Then further conducting the first and second order derivative in both side of Eq. (11), the following two equations can be derived respectively:

$$\begin{aligned}
 & e_N(w) - e_N(w(1 - \frac{a_1}{a_N}))(1 - \frac{a_1}{a_N}) + e_{N-1}(w(1 - \frac{a_1}{a_N}))(1 - \frac{a_1}{a_N}) \\
 & - e_{N-1}(w(1 - \frac{a_2}{a_N}))(1 - \frac{a_2}{a_N}) + \dots + e_1(w(1 - \frac{a_{N-1}}{a_N}))(1 - \frac{a_{N-1}}{a_N}) \\
 & = \frac{E_N(w) + wE_N'(w)}{ba_N}
 \end{aligned} \tag{12}$$

$$\begin{aligned}
 & \sigma_N(w) - \sigma_N(w(1 - \frac{a_1}{a_N}))(1 - \frac{a_1}{a_N})^2 + \sigma_{N-1}(w(1 - \frac{a_1}{a_N}))(1 - \frac{a_1}{a_N})^2 \\
 & - \sigma_{N-1}(w(1 - \frac{a_2}{a_N}))(1 - \frac{a_2}{a_N})^2 + \dots + \sigma_1(w(1 - \frac{a_{N-1}}{a_N}))(1 - \frac{a_{N-1}}{a_N})^2 \\
 & = \frac{2E_N'(w) + wE_N''(w)}{ba_N}
 \end{aligned} \tag{13}$$

where $e_i(w)$ and $\sigma_i(w)$ ($i=1,2..N$) represent unit energy consumption and bridging stress of fictitious crack section which experiences fatigue load for i cycles, separately. If further assumption is made that at any equilibrium state, the stress value at the point of intersection between each section is continuously distributed, which means that the following relation is obtained:

$$\sigma_N(w(1 - \frac{a_i}{a_N})) = \sigma_{N-1}(w(1 - \frac{a_i}{a_N})) \quad \text{for } i=1,2,..N \tag{14}$$

Then finally the equation can be arranged as:

$$\sigma_N(w) = \frac{2E_N'(w) + wE_N''(w)}{ba_N} \tag{15}$$

where b is the width of composite beam.

Substitute the Eq. (2) into Eq. (15). The fictitious crack length a_i , crack mouth opening displacement (CMOD) w and energy applied by external load E_i ($i=1,2..N$) after i cycles of load can be obtained from experiment observation. The values of parameter k_1 and k_2 could be obtained based on data fitting.

4. EXPERIMENTAL OVERVIEW

4.1 Materials and specimens

The w/c ratio and strength properties of concrete and PCM used in this study can be found in Table.1. The PCM used in this study is premixed PAE (polyacrylate acid ester) powder resin and developed as a splaying mortar for a repairing of a cross section of structures. It has characteristics of high density, high bond strength and low contraction. The comparison of durability

Table .1 Material Properties

Material	Water cement ratio	Compressive strength (MPa)	Young's Modulus (GPa)
Concrete	63%	29.29	26.77
PCM	13.40%*	57.23	23.46

*the value of $w/compound$

Table .2 Comparison of Durability between PCM and Normal Mortar

Durability examination	Mortar W/C=50%	PCM W/compound=13.4%
Freezing and Thawing	Relative dynamic elastic Modulus df=86.4% (300 cycle)	Relative dynamic elastic Modulus df=98.5% (300 cycle)
Carbonation	Carbonated thickness 7.4mm (28 days)	Carbonated thickness 0.7 mm(28 days)
Dry shrinkage	6.90E-06	5.52E-06
Chloride ion penetration depth	10mm (28 days)	5.4mm (28 days)

behaviors between PCM and normal mortar is shown in Table.2.

The concrete substrates surfaces are treated by water jet (WJ) method. Special attention was paid to provide adequate moisture on the substrate concrete surface. The substrate concrete was placed in water for 48hrs and free water was removed before casting PCM. The connected interface is separated with wooden triangular prism to induce the notch and the age of specimen at testing is at least three months so as to alleviate the effect of initial hydration development.

4.2. Apparatus and test procedure

(1) Splitting tensile test

The splitting tensile test is used worldwide to measure the tensile strength of concrete. It was first proposed by Lobo Carneiro and Barcellos during the Fifth Conference of the Brazilian Association for Standardization in 1943¹³⁾ and was later adopted as a standard test. Ramey and Strickland¹⁴⁾ used the ASTM C496 standard test method as a general guide and developed a splitting test for composite cylinders, constructed with one-half concrete and one-half repair material. Their test showed that the cylindrical splitting tensile gave consistent results.

In this study, splitting tensile test as shown in Fig.2 was conducted to evaluate the tensile strength of the PCM-concrete interface. To prevent local failure in compression at the loading generators, two thin strips made of plywood are placed between the loading platens and the specimen to distribute the load. A notch with size of 0.75 x 10 cm at each side is induced during the PCM casting procedure. The contact area between the concrete substrate and the PCM is

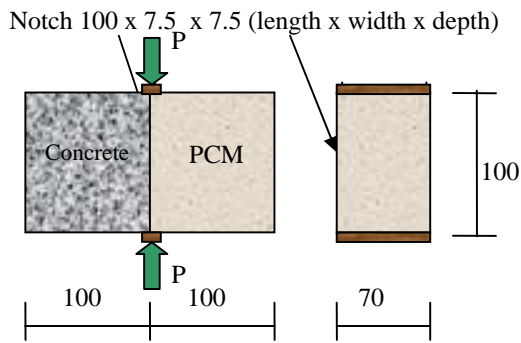


Fig.2 Splitting tensile test setup(unit:mm)

10×5.5 cm. The maximum tensile stress can be calculated by the following equation:

$$\sigma_{\max} = \frac{2P}{\pi A} \quad (16)$$

where σ_{\max} is the maximum tensile strength in the specimen when the applied load is P , A is the area of contacting surface.

(2) Three point bending test

The 50kN capacity feed back controlled loading machine is employed in this study. For static test, the

tests were carried out under displacement control condition and the loading speed was 0.1mm/min. while the fatigue tests were under load control condition. Three point fatigue bending tests were conducted both under static loading and fatigue loading. The detail of experiment set-up of static test can be found in the reference¹⁸⁾. The experimental set-up of fatigue test is shown in Fig. 3.

Static flexure tests were conducted before fatigue flexure tests to determine the static flexure strength. Based on the average flexure strength, the maximum fatigue stress were determined for each level. Since test data of each cycle is used as input, the time and calculation efficient option is to choose a higher value of stress level. In this study, two levels of $S_{\max}=0.90$ and $S_{\max}=0.85$, with one specimen for each level, which the fatigue life are only in hundreds, were conducted.

Fatigue loading was controlled with constant amplitude between maximum and minimum load levels. A frequency of 5 Hz was chosen with a sine wave form. The value of 0.05kN corresponding to the preload was chosen for the minimum load in order to avoid any slip of specimens that can occur under a total unloading in the fatigue test.

4.3 Data collection

For fatigue loading test, Linear Variable Differential Transducers (LVDTs) were introduced to measure the deflection at the mid-span of specimens from both sides of

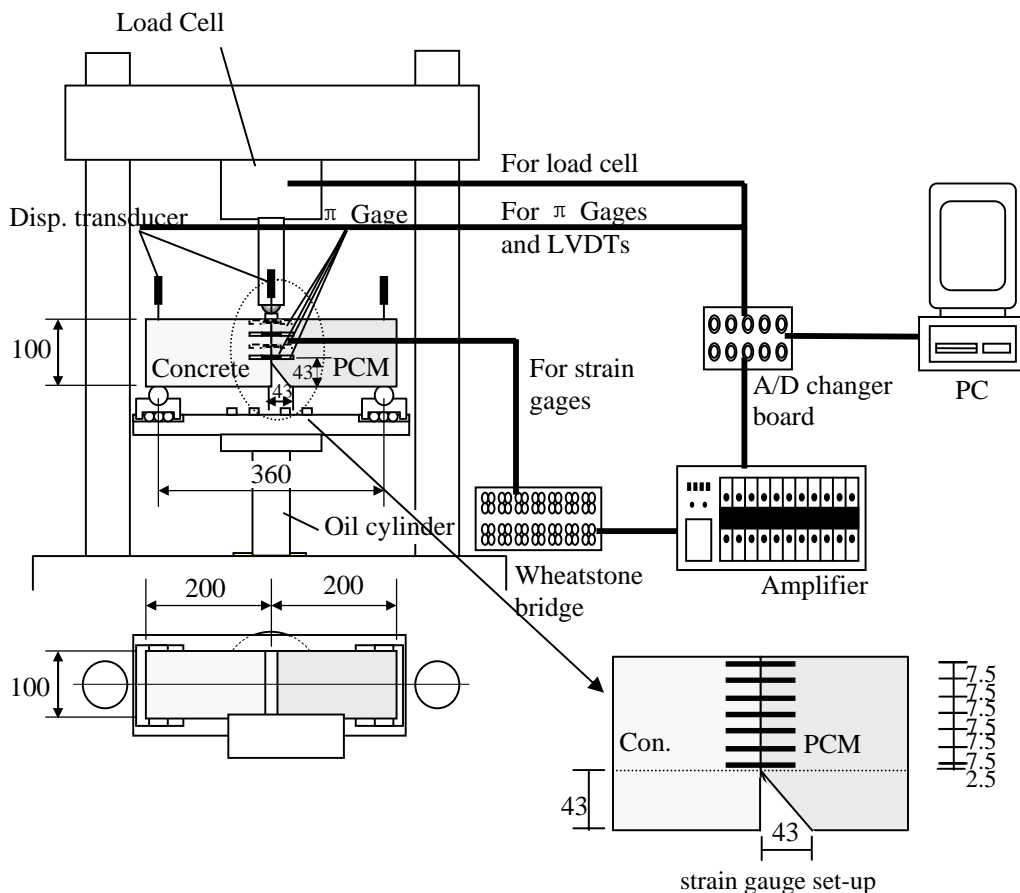


Fig.3 Test set-up of fatigue bending test (unit: mm)

Table.3 Strength of Static Loading Test

Series	1	2	3	Average
Flexural Strength (MPa)	4.78	4.64	4.44	4.62
Tensile Strength (MPa)	2.99	2.81	3.27	3.02

specimens. To obtain the CMOD as well as crack propagation process at the last failure cycle, four one directional π gauges with accuracy of 0.001mm were arranged with the same distance from the position of notch tip to the top of composite beam. To evaluate the propagation of the fictitious crack in the ligament portion, the longitudinal strain distribution of the notched beam was measured. Strain gauges with length of 5mm were provided along the ligament portion. For the purpose of obtaining as many measured data as possible to evaluate the fictitious crack propagation, seven strain gauges were placed on the ligament portion. Each strain gauge was set 7.5mm apart as shown in Fig.3.

The 100Hz sampling system “ADREC” consisting of Wheatstone bridge, amplifier, A/D changer board and personal computer was used for recording the data. 100 samples could be measured for 1 second by using this system. The set-up of this system is schematically shown in Fig .3.

5. EXPERIMENTAL RESULTS AND ANALYSIS

The experimental results under both static and fatigue loading are illustrated and discussed in this section.

5.1. Results under static loading

The relation between load and mid-span deflection of three static specimens of composite beam are shown in Fig. 4. The ultimate tensile strength and flexural strength of composite specimens is shown in Table 3. The average

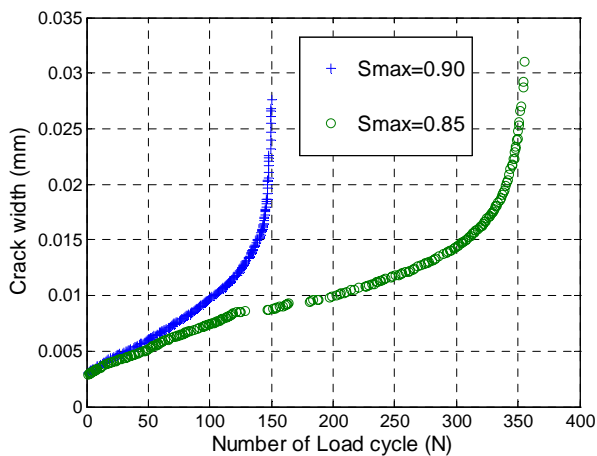


Fig.5 Crack evolution curve

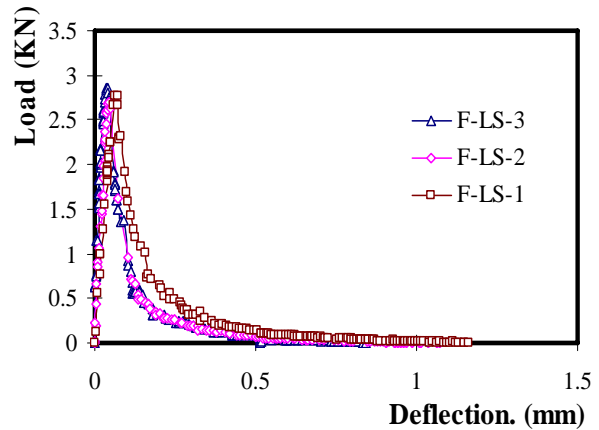


Fig.4 Load-deflection relation under static loading

flexural strength is used to determine the fatigue stress in the fatigue test.

5.2. Results under fatigue loading

Fatigue test results are used for determining the bridging stress degradation relation. In the calculating procedure, several essential material relations, the constitutive relation under static loading, the energy applied by external load and the development of fictitious crack and central deflection based on experimental results, are introduced as input in the equation.

(1) Damage characteristics

The progressive fatigue failure is described by illustration of increase in CMOD against the number of cycles as shown in Fig. 5.

It can be seen that the failure characteristics of PCM-concrete interface is similar to those of cementitious material like concrete and can be divided into two distinct stages. The first stage is the deceleration stage, where the rate of damage of a specimen decreases as the crack grows at a small number of loading cycles. The second stage is an acceleration stage, where there is steady increase in the crack growth rate right up to failure. On a certain degree, the failure characteristics of

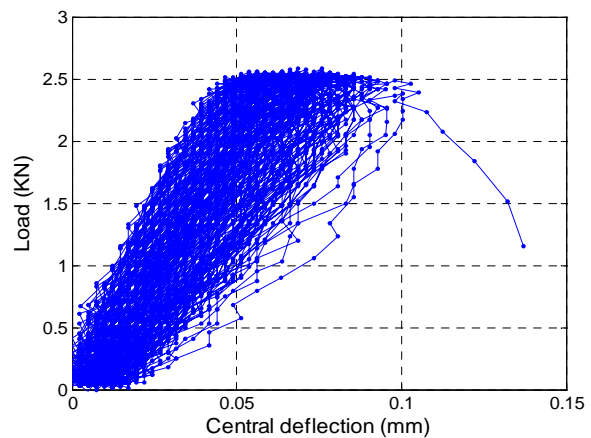


Fig.6 Load-Deflection relation under fatigue loading ($S_{max}=0.9$)

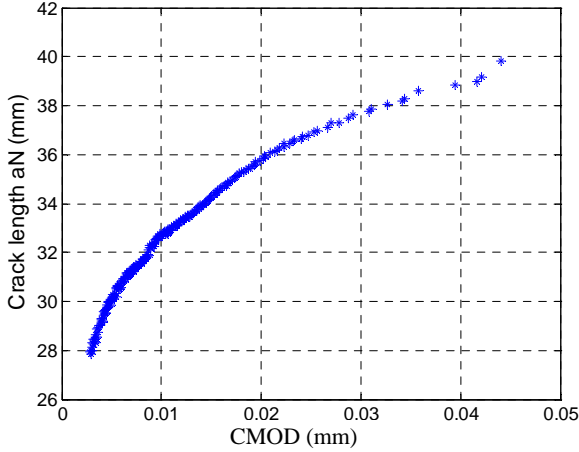


Fig.7 Crack length and CMOD relation ($S_{max}=0.90$)

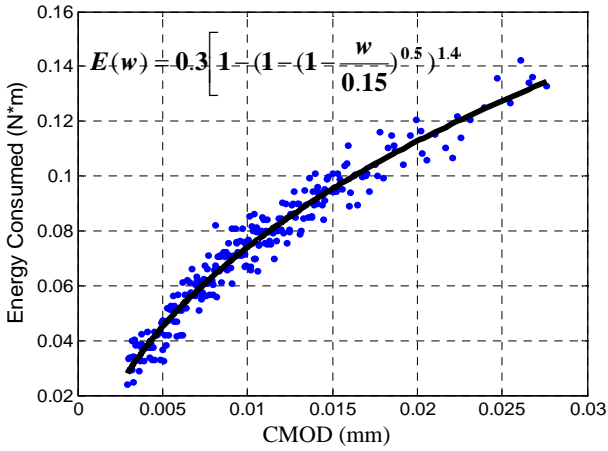


Fig.8 $E(w)$ – CMOD relationship ($S_{max}=0.90$)

PCM-concrete interface observed in this test further demonstrates the validity of assumption that PCM-concrete interface performs like cementitious materials.

(2) Load-deflection curves

Fig.6 exhibits a typical load-deflection curve until total failure of specimen as obtained from flexural fatigue test. It can be noticed that by using “ADREC” system, the load-deflection relation of each cycle can be recorded.

(3) Fictitious crack propagation

The crack opening calculated from the output from seven strain gauges disposed at the ligament portion is assumed to be fictitious CMOD. The tip of fictitious crack at maximum load of each cycle corresponds to the point at which the strain is zero and the length of fictitious crack can be obtained and plotted against CMOD in Fig.7.

5.3 Implementation and Discussion

In this section, the bridging degradation law is calculated using the procedure of fatigue analysis discussed in Chapter 3. The calculation procedure consists of two stages:

In the first stage, the calculation of the energy applied by the external load after a certain number of cycles of fictitious loading is performed. The result is shown in Fig.8.

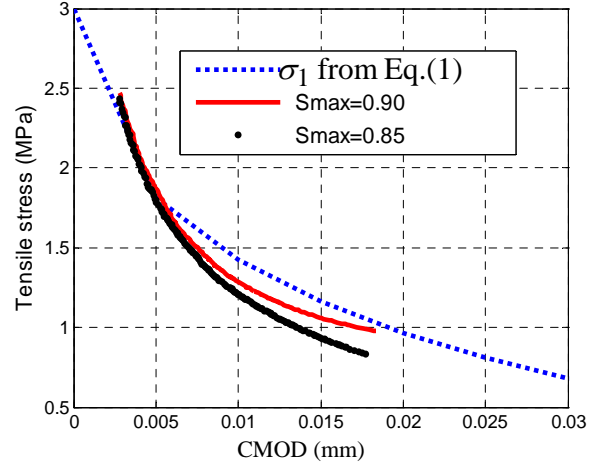


Fig.9 Tensile stress-CMOD relationship

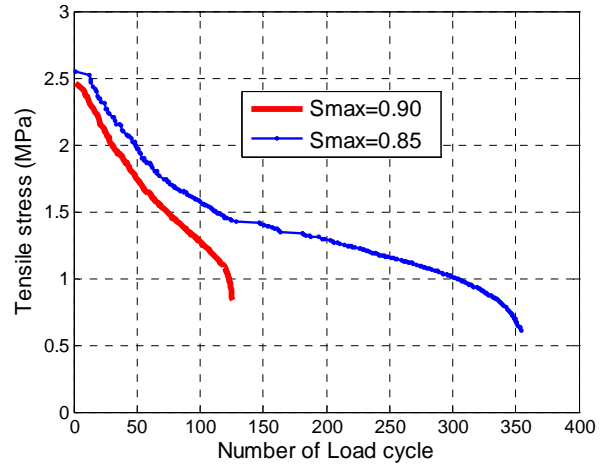


Fig.10 Stress-Number of cycle relation

In order to avoid the influence of data fluctuation, the relation between energy consumed and CMOD is firstly represented by a mathematical expression based on data fitting method. Then the first order and second order derivative calculation is conducted together with input of fictitious CMOD and length obtained from test results to determine the value on the right side of Eq.(15). The calculation result is plotted against CMOD and number of loading cycles in Fig .9 and Fig. 10 respectively. It can be seen from Fig. 9 that for the same CMOD, the tensile stress when $S_{max}=0.85$ is smaller than tensile stress when $S_{max}=0.9$. This is because it experiences more load cycles to reach the same CMOD and subsequently has more stress degradation.

In the second stage, the bridging degradation law as shown in Eq.(2) is substituted into left side of Eq.(15) and the value of k_1 and k_2 can be obtained through two-parameter nonlinear fitting method. The final degradation relation derived from combined data of two stress levels for PCM-concrete interface is shown below:

$$\frac{\sigma_N}{\sigma_1} = 1 - (0.098 + 3.32w) \log N \quad \text{for } w \leq 0.016\text{mm}$$

$$\frac{\sigma_N}{\sigma_1} = 1 - (0.12 + 1.2w) \log N \quad \text{for } w > 0.016\text{mm} \quad (17)$$

In order to compare the stress degradation relation between normal concrete and PCM-concrete interface, the stress degradation relation of concrete obtained by cyclic uniaxial tensile tests¹⁷⁾ is quoted in this study and expressed as follows:

$$\frac{\sigma_N}{\sigma_1} = 1 - (0.08 + 4w) \log N \quad \text{for } w \leq 0.016\text{mm}$$

$$\frac{\sigma_N}{\sigma_1} = 1 - (0.14 + 0.12w) \log N \quad \text{for } w > 0.016\text{mm}$$

(18)

It is noticed that the coefficient k_1 and k_2 in the degradation law of PCM-concrete interface are similar to that of normal concrete when crack width is smaller than 0.016mm, while k_2 for PCM-concrete interface is larger than for normal concrete when crack width is larger than 0.016mm. This implies that PCM-concrete interface exhibits the higher rate of bridging stress degradation than that of aggregate bridging in normal concrete, and should be regarded as the key issue of PCM retrofitted structures especially subjected to fatigue loading.

6. CONCLUSIONS

A fatigue analysis method of PCM-concrete composite beam under fatigue flexure has been proposed by applying the concept of bridging effect degradation and fictitious crack based on theory of energy equivalence. The analytical method has been developed based on the fatigue failure mechanism of PCM-concrete interface that is governed by crack propagation as the result of interface bridging degradation. The J-integral method proposed for determining the tension softening relation of concrete under static loading is modified to determine the PCM-concrete interface tensile stress degradation relation. This method has the following features:

- (1) Theoretically speaking, the tensile stress degradation relation can be determined from a single beam specimen.
- (2) Only the load, the load point displacement, the crack length and opening width are necessary to be measured or determined. Meanwhile, the fatigue bending test is easier to be performed than the uniaxial tensile fatigue test.
- (3) The method proposed in this study can be used for other cementitious materials or composite interfaces as long as the theory of fictitious crack and energy equivalence are tenable.
- (4) The PCM-concrete interface stress degradation relation was obtained based on the method mentioned above and compared with that of crack in normal concrete. It can be found that the PCM-concrete interface has higher degradation rate so that more attention should be paid to the PCM-concrete interface during the design of PCM-retrofitted structures under fatigue loading.

ACKNOWLEDGEMENT

The surface WJ treatment work described in this paper was carried out at Hokusei Kensetsu Co.Ltd. The authors are grateful to their collaboration.

REFERENCES

- 1) Tran, Q. T., Toumi, A. and Turatsinze, A., Modelling of debonding between old concrete and overlay: fatigue loading and delayed effects, *Materials and Structures*, DOI 10.1617/s11527-006-9204-y.
- 2) Ohama, Y., Recent progress in Concrete-Polymer composites, *Advanced Cement Based Materials*, Vol.5, No.2, pp. 31- 40,1997.
- 3) Peerapong, S. and Takashi, M., Fiber bridging degradation based fatigue analysis of ECC under flexure, *Journal of Applied Mechanics* Vol.6 pp. 1179-1188 (August 2003).
- 4) Li, V.C. and Ward, R.J.:. A novel testing technique for post-peak tensile behavior of cementitious materials, *Fracture Toughness and Fracture Energy*, Balkema, 183-195, 1989.
- 5) Rokugo, K., Iwasa, M., Seko, S. and Koyanagi, W., Tension softening diagrams of steel fiber reinforced concrete, *Fracture of Concrete and Rock*, Elsevier, 513-522, 1989.
- 6) Uchida, Y., Rokugo, K. and Koyanagi, W., Determination of tension softening diagrams of concrete by means of bending test. *Journal of Materials, Concrete Structures and Pavements of JSCE*, No.426/V-14, 203-212, 1991.
- 7) Niwa, J. ,Sumranwanich and Tantermisirikul, S.: New Method to Determine the Tension Softening Curve of Concrete, *Fracture Mechanics of Concrete Structures*. Proceedings of FRAMCOS-3, Vol.1, 347-356, 1998.
- 8) Neville, A. M, and Brooks, J.J, *Concrete technology*, Longman Scientific & Technical, London.
- 9) Zhang, J., Stang, H., and Li, V.C, Experimental study on crack bridging in FRC under uniaxial fatigue tension, *J. Mat. In Civ. Engrg.*, ASCE, 12(1), 66-73, February 2000.
- 10) Hillerborg, A., Modeer, M. and Petersson, P.-E. 1976. Analysis of crack formation and crack growth in concrete by means of fracture mechanics and finite elements, *Cement and Concrete Research*, Vol.6. pp. 773-782, 1976.
- 11) Dawei, Z., Furuuchi, H., Hori, A., Fujima, S. and Ueda, T., Influence of interface roughness on PCM-concrete interfacial fracture parameters, Proceedings of the third ACF International Conference, 11-13 November 2008, HCM City.
- 12) JIS B 0601:Geometrical Product Specifications (GPS) - Surface texture: Profile method- Terms, Definitions and surface texture parameters, JIS,2001.1
- 13) Lobo Carneiro, F. Barcellos, A., Resistance a la Traction des Betons, *Int. Assoc. Test. Res. Lab. Mater. Struct.* RILEM Bull. 13 (1949) 98-125.
- 14) Ramey, G.E., Strickland, A.M., An experimental evaluation of rapid setting patching materials used in the repair of concrete bridges and pavements, Alabama

Highway Research, Project 930-103, Part II, 1984, pp. 48– 56.

- 15) Gopalaratnam, V.S., and Shah, S.P., Softening response of plain concrete in direct tension. *ACI J.*, 82(3), 310-323.
- 16) Reinhardt, H. W., Cornelissen, A. W., and Hordijk, D.A., Tensile tests and failure analysis of concrete, *J. Struct. Engrg.*, ASCE, 112(11), 2462-2477.
- 17) Hordijk, D.A., Tensile and tensile fatigue behaviour of concrete, experiments, modeling and analyses, *Heron*, 37(1), 1- 77, 1992.
- 18) Dawei, Z., Furuuchi, H., Hori, A. and Ueda, T., Mode I Fracture Behaviors of PCM-concrete Interfaces, *Proceedings of JCI*, Vol.30, No.2, 2008.